Aalborg Universitet

Vector-Norm Based Truncation of Harmonic Transfer Functions in Black-Box Electronic Power Systems

Liao, Yicheng; Sandberg, Henrik; Wang, Xiongfei

Vector-Norm Based Truncation of Harmonic Transfer Functions in Black-Box Electronic Power Systems

YICHENG LIAO [1] **(Member, IEEE), HENRIK SANDBERG** [2] **(Senior Member, IEEE),
AND XIONGFEI WANG** [2,3] **(Senior Member, IEEE)**

[1]Elnetanalyse, Energinet, 7000 Fredericia, Denmark
[2]School of Electrical Engineering and Computer Science, KTH Royal Institute of Technology, 100 44 Stockholm, Sweden
[3]AAU Energy, Aalborg University, 9220 Aalborg, Denmark

CORRESPONDING AUTHOR: XIONGFEI WANG (e-mail: xwa@energy.aau.dk)

ABSTRACT Power systems equipped with power electronic converters can be modeled by harmonic transfer functions (HTFs) in a black-box manner for dynamic analysis. This paper studies the truncation of HTFs. It is proposed to define the gain function of an HTF as the norm of its central-column vector. Then, the error bound of the gain function in relation to the truncation order is explicitly derived, which can be used as an indicator for the HTF truncation. Compared with existing solutions, the proposed method is practical in truncating black-box systems with unknown internal parameters, since the truncation error bound can be estimated by the central-column elements of the HTF, which can be easily measured through frequency scan. The truncation approach is finally verified on a three-phase electronic power system by electromagnetic transient simulations.

INDEX TERMS Time-periodic system, harmonic transfer function, truncation, frequency scan, black-box system, frequency-domain analysis.

I. INTRODUCTION

Linearized modeling has been widely applied for dynamic analysis of electronic power systems [1]–[5]. These systems feature time periodicity under alternating-current (AC) operations, which can be linearized around their periodic trajectories [6]. Then, harmonic state-space (HSS) models or harmonic transfer functions (HTFs) can be used to characterize the dynamic behaviors of the linear time-periodic (LTP) system [7]. These approaches enable the small-signal analysis of frequency-coupling dynamics of electronic power systems in the frequency domain. However, the converter systems are usually black-box systems due to their control confidentiality. HTFs are thus more feasible than the HSS models, since they can directly characterize the system's dynamics from the input-output perspectives, even without knowing the internal control details. Moreover, the HTFs can be obtained easily by the frequency-scan measurement [8], [9] and further used for stability analysis based on the Nyquist stability criterion [9]–[12].

Theoretically, the HTF is an infinite-order matrix operator, since its input and output are represented by Fourier coefficients of time-periodic variables, which may consist of infinite elements. In practice, since the system operating conditions only involve certain harmonic components, such as in unbalanced or harmonically distorted grids, the HTF can be truncated into a finite-order matrix operator. It is thus important to select a truncation order of HTFs prior to dynamic studies.

The conventional approach to the HTF truncation order selection usually considers the dominant harmonic components in the system steady states, such as in unbalanced grids [8], [13], [14] and in modular multilevel converter-based systems [12], [15]. However, the harmonic level can vary from case to case, and the HTF also depends on the entire system dynamic model including control dynamics. It is thus not rigorous to simply use the harmonic level as a reference for the HTF truncation.

There are several rigorous approaches to the HTF truncation. The first approach is based on the harmonic state-space

(HSS) modeling of LTP systems. The truncation order needs to ensure that the eigenvalue errors between the infinite-order HSS model and the truncated HSS model is sufficiently small, such that all the eigenvalues appear in the fundamental strip on the complex plane [7], [16]–[18]. However, this approach usually results in unnecessarily high truncation orders, since it does not consider how fast the model converges as the truncation order increases. To overcome the conservatism of the aforementioned method, a truncation order selection method based on the time-domain responses of LTP eigenvectors was proposed, which defined an L_1-norm to quantify the truncation error between the actual LTP eigenvectors and the approximated responses from the truncated model [19]. The truncation order can be determined when the error is smaller than a predefined threshold.

Alternatively, the truncation can be done directly based on the HTFs. There are several HTF truncation methods, i.e., the skew truncation [20], the square/rectangular truncation [21], [22], and the skew-rectangular truncation [23]. These truncation methods use different norms to quantify the truncation error, and the error bounds can be calculated based on the convergence rates, known as roll-offs. More specifically, the skew truncation retains the major skew diagonals and neglects other diagonals, which still yields an infinite-order operator of the HTF, yet makes it easier to prove the convergence since the system's gain can be defined based on H_2-norm [20], [22]. The rectangular truncation considers certain harmonic orders in the input and output signals, which results in a finite-order rectangular matrix as the truncated HTF and is thus simpler for numerical calculations. The rectangular truncation utilizes the H_∞-norm to quantify the truncation error [22]. The skew-rectangular truncation is the combination of skew and rectangular truncations [23], which keeps their advantages. For these truncation methods, the truncation order can also be determined if the error bound is smaller than a predefined threshold.

However, the existing approaches to the HTF truncation mainly rely on a prior knowledge of an explicit system model or some important parameters, which cannot be easily obtained in black-box systems. The HSS or LTP eigenvector based approach needs to formulate the system model with the state-space representation. However, the internal state variables in converter systems are usually unknown due to the confidentiality of converter controls, which thus require much more efforts on computing a state-space realization [24]. The HTF-based truncation methods require knowing the system skew roll-off or input and output roll-offs to estimate the truncation error bounds, which are also unknown for a black-box system. Although the HTF could be measured by frequency scan and the error bounds could be estimated based on the H_∞-norm calculation, a complicated identification of all the elements in a sufficiently large HTF matrix is needed [22], which is still complex.

This work thus aims to develop a more practical HTF truncation method for "black-box" systems. First, the gain function of an HTF is defined by the norm of its central-column

vector. The so-defined gain function can be used to generalize the bandwidth concept of LTI systems to LTP systems. Then, the truncation error bound is derived based on the gain function. The HTF truncation order can be determined by setting a threshold to the truncation error bound. The developed truncation approach allows for determining the truncation order simply using the measured frequency responses considering a single-frequency input, which is thus more appealing than the existing methods from a practical standpoint. The theory is finally validated on a three-phase converter-based power system through electromagnetic transient (EMT) simulations.

II. VECTOR-NORM BASED TRUNCATION

The vector-norm based truncation method is proposed in this section. The basic concepts of LTP systems and HTFs are reviewed first in Part A. Then, the gain function of a single-input single-output (SISO) LTP system[1] is defined in Part B, based on which, the truncation error bound is derived in Part C. Then, how to extend the truncation analysis to a multiple-input multiple-output (MIMO) LTP system is introduced in Part D. To facilitate the application of this approach for black-box systems, its practical implementation is introduced in Part E. Finally, the advantages of the proposed approach are highlighted by comparisons with other truncation methods in Part F, and the relationship between the proposed approach and the skew truncation is also discussed.

A. LINEAR TIME-PERIODIC SYSTEM AND HARMONIC TRANSFER FUNCTION

An LTP system can be represented in the state-space form as

$$\dot{x}(t) = A(t)x(t) + B(t)u(t)$$
$$y(t) = C(t)x(t) + D(t)u(t) \quad (1)$$

where all the coefficient matrices $(A(t), B(t), C(t), D(t))$ are time periodic with the fundamental period of $T = 2\pi/\omega_p$. All the variables $(x(t), u(t), y(t))$ can be represented by exponentially modulated periodic signals with the form of

$$x(t) = e^{st} \sum_k x_k e^{jk\omega_p t} \quad (2)$$

where $s \in \mathbb{C}$ such that e^{st} can introduce frequency-dependent dynamics, and similarly for $u(t)$ and $y(t)$. Then, based on the Fourier series expansion and the harmonic balance, the HSS model can be derived to characterize the frequency-domain response of an LTP system [7], which is represented by

$$s\boldsymbol{x} = (\boldsymbol{\mathcal{A}} - \boldsymbol{\mathcal{N}})\boldsymbol{x} + \boldsymbol{\mathcal{B}}\boldsymbol{u}$$
$$\boldsymbol{y} = \boldsymbol{\mathcal{C}}\boldsymbol{x} + \boldsymbol{\mathcal{D}}\boldsymbol{u} \quad (3)$$

In (3), the variable dynamics are represented by their Fourier coefficients given by $\boldsymbol{x} = [\dots, x_{-k}, \dots,$

---

[1]SISO LTP system means that the frequency-domain inputs and outputs of the HTF correspond to single input and single output in the time domain. MIMO LTP system means that the frequency-domain inputs and outputs of the HTF correspond to multiple inputs and multiple outputs in the time domain.
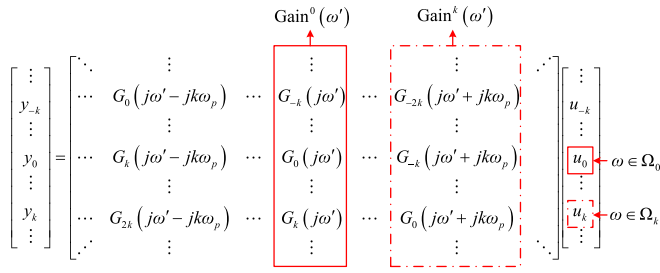
FIGURE 1. Gain function definition of an HTF considering single-frequency input.

FIGURE 2. Gain function of an HTF shown on magnitude Bode diagram.

$x_0, \ldots, x_k, \ldots]^T$, similarly for $\boldsymbol{u}$ and $\boldsymbol{y}$. The time-periodic coefficients are represented by block Toeplitz matrices, whose elements are also obtained from their Fourier coefficients. $\boldsymbol{\mathcal{N}}$ is a diagonal matrix defined as

$$\boldsymbol{\mathcal{N}} = diag\left\{ \cdots -jk\omega_p \cdots 0 \cdots jk\omega_p \cdots \right\} \qquad (4)$$

In such a way, the HTF model from $\boldsymbol{u}$ to $\boldsymbol{y}$ can be derived to represent the frequency response of the LTP system, i.e.,

$$\boldsymbol{G}(s) = \boldsymbol{C}[s\boldsymbol{I} - (\boldsymbol{A} - \boldsymbol{\mathcal{N}})]^{-1}\boldsymbol{B} + \boldsymbol{D} \qquad (5)$$

Theoretically, the HTF should be an infinite-order matrix, which can be represented by

$$\boldsymbol{G}(s) = \begin{bmatrix} \ddots & \ddots & \ddots & \ddots & \ddots \\ \ddots & G_0(s - j\omega_p) & G_{-1}(s) & G_{-2}(s + j\omega_p) & \ddots \\ \ddots & G_1(s - j\omega_p) & G_0(s) & G_{-1}(s + j\omega_p) & \ddots \\ \ddots & G_2(s - j\omega_p) & G_1(s) & G_0(s + j\omega_p) & \ddots \\ \ddots & \ddots & \ddots & \ddots & \ddots \end{bmatrix} \qquad (6)$$

The HTFs are defined within the fundamental frequency interval for which $\text{Im}(s) \in \Omega_0 := [-\omega_p/2, \omega_p/2]$, since the response of an LTP system beyond the fundamental frequency interval can always be folded into Ω_0.

B. GAIN FUNCTION OF LTP SYSTEMS

The conventional HTF is defined for harmonic input within the fundamental frequency interval Ω_0. Actually, if interpreted from the space of input signals, an LTP system may have a harmonic input at any frequency even beyond Ω_0. Therefore, a new gain function of an LTP system is defined considering the harmonic input frequency of $\omega \in \mathbb{R}$. It is assumed that the HTF is defined for $\omega' \in \Omega_0$, then the response of the system is discussed as follows considering different frequency intervals where ω belongs.

1) $\omega = \omega' \in \Omega_0$

If the input frequency is within the fundamental frequency interval Ω_0, the frequency response is determined by the central-column vector of the HTF, corresponding to the input of u_0, as shown in the solid box in Fig. 1. Then, the gain
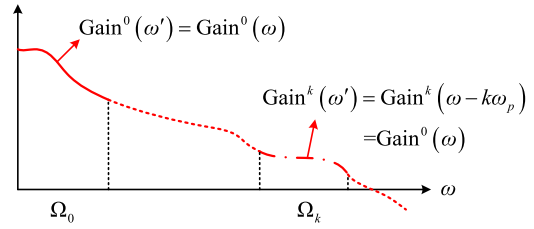
function can be defined as the norm of this vector, i.e.,

$$\text{Gain}(\omega) = \text{Gain}^0(\omega') := \left\| \begin{matrix} \vdots \\ G_{-k}(j\omega') \\ \vdots \\ G_0(j\omega') \\ \vdots \\ G_k(j\omega') \\ \vdots \end{matrix} \right\| \quad \text{for } \omega \in \Omega_0 \qquad (7)$$

2) $\omega = \omega' + k\omega_p \in \Omega_k$

If the input frequency is within the k-th frequency interval Ω_k, where k is a non-zero integer, the frequency response is determined by the corresponding column vector of u_k, as shown in the dash-dot box in Fig. 1. The gain function can thus be defined as

$$\text{Gain}(\omega) = \text{Gain}^k(\omega') := \left\| \begin{matrix} \vdots \\ G_{-2k}(j\omega' + jk\omega_p) \\ \vdots \\ G_{-k}(j\omega' + jk\omega_p) \\ \vdots \\ G_0(j\omega' + jk\omega_p) \\ \vdots \end{matrix} \right\| \quad \text{for } \omega \in \Omega_k$$

$$(8)$$

Considering the separate definitions of the gain function in different frequency intervals, the magnitude Bode diagram of the gain function can be plotted in Fig. 2, where only the fundamental and positive frequency intervals are shown for simplicity. The negative frequency intervals can be derived and plotted similarly.

It can be easily derived from (7) and (8) that

$$\text{Gain}^k(\omega') = \text{Gain}^k(\omega - k\omega_p) = \text{Gain}^0(\omega) \qquad (9)$$

Consequently, the gain function of an LTP system considering the single-frequency input can be simply defined based on the central-column vector of the HTF, i.e.,

$$\text{Gain}(\omega) := \text{Gain}^0(\omega) \quad \text{for } \forall \omega \in \mathbb{R} \qquad (10)$$

This gain function implies the total harmonic responses in the output with the injection of a single harmonic in the input,

which is simple for interpretation. It can thus be used to define the bandwidth of an LTP system. If $\mathcal{G}$ represents an open-loop HTF, the crossover frequency can be defined as the frequency where the magnitude of $\text{Gain}(\omega)$ crosses over 0 dB. If $\mathcal{G}$ represents a closed-loop HTF, the bandwidth can be defined at the frequency where the magnitude of $\text{Gain}(\omega)$ crosses over -3 dB. In such a way, the bandwidth for LTI systems can be generalized to LTP systems.

Based on the gain function, the gain of a truncated HTF with the order of N can be formulated as

$$\text{Gain}_N(\omega) := \text{Gain}_N^0(\omega) = \left\| \begin{array}{c} G_{-N}(j\omega) \\ \vdots \\ G_0(j\omega) \\ \vdots \\ G_N(j\omega) \end{array} \right\| \qquad (11)$$

It is noted that this gain function is only used for truncation error analysis. When it comes to dynamical analysis, the matrix-form HTF needs to be constructed with the given truncation order of N, since the system may have multiple frequency inputs. The HTF form can be chosen by either skew truncation or rectangular truncation, since their truncated HTFs have the same gain function defined by the central-column vectors.

C. TRUNCATION ERROR BOUND

Based on the gain function, the truncation error can be defined as

$$e_N(\omega) := \text{Gain}_\Delta(\omega) \big/ \text{Gain}_N(\omega)$$

$$\text{where } \text{Gain}_\Delta(\omega) := \text{Gain}_\Delta^0(\omega) = \left\| \begin{array}{c} \vdots \\ G_{-(N+1)}(j\omega) \\ G_{N+1}(j\omega) \\ \vdots \end{array} \right\| \qquad (12)$$

The truncation error is an important index to perform the truncation analysis. The truncation can stop if the truncation error is smaller than an accepted threshold.

It can be seen from (12) that the truncation error depends on how small $\text{Gain}_\Delta(\omega)$ is, which is calculated by infinite number of elements, and is impossible to be obtained in practice. To tackle this challenge, a truncation error bound can be estimated as

$$e_N(\omega) \le \varepsilon_N(\omega) := \frac{\|g_{N+1}(\omega)\|}{\text{Gain}_N(\omega)} \cdot \sqrt{\frac{1}{1 - \varepsilon^2}}$$

$$\text{if } \frac{\|g_{k+1}(\omega)\|}{\|g_k(\omega)\|} \le \varepsilon < 1 \text{ for } \forall k \ge N + 1 \text{ and } \forall \omega$$

$$\text{where } \|g_k(\omega)\| := \sqrt{|G_{-k}(j\omega)|^2 + |G_k(j\omega)|^2} \qquad (13)$$

whose proof is given in Appendix A.

It should be noted that $\varepsilon < 1$ in (13) is an assumption made to quantify the error bound in a simple way. It is similar to the assumption of system roll-offs [22] that ensure a decay rate of the higher-order harmonics such that the norm will converge. Theoretically, ε should be the upper bound of $\| g_{k+1} \|/g_k$ for $\forall k \ge N + 1$. However, in practice, it is impossible to calculate all the infinite harmonic responses ($\| g_k \|$) in the measured output response to obtain this upper bound ε. Only some finite number of harmonic responses can be measured reliably, since some higher-order harmonic responses can be too low to be detected. Then, an upper bound ε can be estimated based on the finite-order harmonic responses. If the aforementioned assumption holds, the error bound can be calculated by (13) and used for truncation analysis.

D. EXTENSION TO MIMO LTP SYSTEMS

The gain function defined by the central-column vector for truncation analysis applies to SISO LTP systems. If the HTF characterizes the dynamics of a MIMO LTP system, the entire HTF can be seen as composed of block HTFs of multiple SISO LTP systems. Then, the gain function can be defined by the Frobenius norm of a matrix that is composed of the central-column vectors of all the block HTFs. Here, the Frobenius norm is chosen instead of the maximum singular value, since it can be easily used to define the truncation error and estimate the error bound based on (12) and (13), by considering the elements of different harmonic orders. The application to a MIMO LTP system will be elaborated explicitly in the case studies.

E. IMPLEMENTATION OF THE PROPOSED TRUNCATION APPROACH

The proposed method can be used to truncate the HTFs of black-box systems, which requires to first measure the frequency responses of the central-column vector of the HTF. The measurement can be easily done by the frequency scan, which includes the following steps.
- First, the input and output of the black-box system are defined and the steady state of the input is extracted.
- Next, a single-frequency perturbation is injected and superimposed on the steady state of the input.
- Then, the frequency responses in the input and output are analyzed by discrete Fourier transformations (DFTs), and the elements in the central-column vector of the HTF can be further calculated.

With the measured central-column vector, the truncation can be implemented in two ways:
- Calculate the gain functions by (11) as the truncation order N increases, then compare them on Bode diagrams. The truncation order can be selected when the convergence is observed. This graphical way is simple and intuitive, yet it cannot quantify the truncation error.
- Estimate the truncation error bounds by (13) as the truncation order N increases. Then, select the truncation order when the error is sufficiently small by comparing with an accepted threshold.

The two ways of truncation analysis will be both implemented in later case studies for cross validation.

TABLE 1 Comparison of Different Truncation Methods for Black-Box LTP Systems

Methods		Need of state-space realization	Numerical feasibility	Ease in computation
HSS eigenvalue analysis [7]		Yes	Yes	+
LTP eigenvector analysis [19]		Yes	Yes	+
HTF skew truncation	Skew roll-off [22]	Yes	Yes	+
	H_2-norm [20]	No	No	−
	Vector-norm based gain function (proposed approach)	No	Yes	+++
HTF rectangular truncation	Input and output roll-offs [22]	Yes	Yes	+
	H_∞-norm [22]	No	Yes	++

Note: In the column of "ease in computation", more "+" denotes less computation effort required for truncating black-box systems. "−" means not applicable since the method is not numerically feasible.

F. COMPARISON AND DISCUSSION

A comparison among different truncation approaches for black-box LTP systems is conducted. Since different methods are based on different principles and follow different procedures, Table 1 is summarized by comparing and discussing their principles and procedures. Three aspects are compared, i.e., need of state-space realization, numerical feasibility, and ease in computation. Then, the relationship between the proposed approach and the skew truncation is further discussed.

1) NEED OF STATE-SPACE REALIZATION

As seen in Table 1, most approaches are conducted based on state-space models. The HSS eigenvalue analysis solves the eigenvalues of the harmonic state matrix of an HSS model, and the LTP eigenvector analysis directly solves the LTP eigenvector of an LTP state-space model in the time domain. The other methods based on skew or input/output roll-offs also need parameters of a state-space model to derive the roll-offs analytically. Thus, if these approaches are used for truncating a black-box system, a prior state-space realization is needed.

In contrast, the norm-based methods are based on the input-output dynamics, thus they can be implemented based on measurement of input and output signals without a state-space realization.

2) NUMERICAL FEASIBILITY

Most of the truncation approaches are numerically feasible. If the state-space realization can be computed numerically, the HSS eigenvalue or LTP eigenvector can be further calculated based on matrix computations and differentiations. The skew and input/output roll-offs can also be calculated based on parameters of the state-space model.

For the norm-based approaches, only the proposed method and the H_∞-norm based method are numerically feasible, because they estimate the norms using finite elements. The proposed method considers finite elements in the central-column vector of an HTF, and the H_∞-norm based method considers the finite elements in a rectangular truncation of an HTF [22]. In contrast, the H_2-norm is defined based on skew truncation, whose truncated HTF operator still has an infinite order [20], [22]; thus, it is infeasible to numerically calculate the H_2-norm.

3) EASE IN COMPUTATION

The truncation approaches that are numerically feasible for black-box systems are further compared based on the ease in computation. The number of "+" is used to represent different levels of computation effort. More "+" denotes less computation effort.

For the state-space based truncation methods, to find a state-space realization for an LTP black-box system is nontrivial and also computationally expensive [24]. Thus, applying these approaches for truncating black-box systems is the most difficult.

The norm-based approaches are easier in computation, since they do not need the state-space realization. They can be conducted by measurement of input and output signals. The H_∞-norm requires to measure all the elements in a rectangularly truncated HTF, which has more computation burden than only measuring the central-column vector by the proposed approach. Therefore, the H_∞-norm based method is more computationally expensive than the proposed method.

4) RELATIONSHIP BETWEEN PROPOSED APPROACH AND SKEW TRUNCATION

The proposed vector-norm based truncation approach can be interpreted as a practical and simple implementation of the skew truncation. The relationship between the vector-norm based truncation and the skew truncation can be derived by the truncation error bound analysis. If there exists a finite error bound $\bar{\varepsilon}_N$ for the gain function based on the central-column vector norm, it can be derived that it also serves an error bound for the skew truncation based on the H_2-norm, i.e.,

$$\|G_\Delta\|_{H_2}^2 := \|G - G_N\|_{H_2}^2 \le \bar{\varepsilon}_N^2 \|G_N\|_{H_2}^2$$

$$\text{where } \bar{\varepsilon}_N := \max_{\omega \in \mathbb{R}} \varepsilon_N(\omega) \tag{14}$$

The proof is provided in Appendix B. The derivation shows that the H_2-norm is bounded by the Frobenius norm of the HTF. Since it is assumed that the truncation error of each column-vector norm is bounded by $\bar{\varepsilon}_N$, the sum of different column-vector norms, which is the Frobenius norm of the HTF, should also be bound by $\bar{\varepsilon}_N$. Thus, the truncation error based on H_2-norm is bound by $\bar{\varepsilon}_N$.
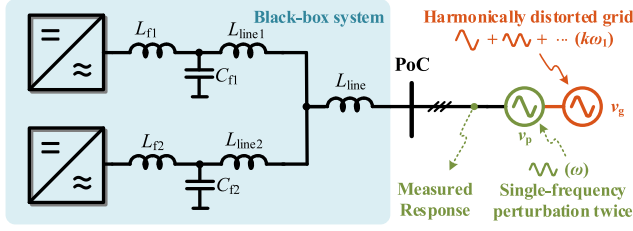
FIGURE 3. The studied power converter-based electrical system.

FIGURE 4. Measured frequency responses of the two column vectors in the admittance HTF.

It is noted that the truncation error analysis based on the central-column vector norm does not necessarily require the Frobenius norm, H_∞-norm or H_2-norm of the HTF to converge. For systems with improper LTI transfer functions, the Frobenius norm, H_∞-norm or H_2-norm of the HTF is unbounded. In such cases, the conventional skew and rectangular truncations that rely on the H_∞-norm or H_2-norm may not work. However, the proposed method can still satisfy the convergence of central-column vector norm.

III. CASE STUDIES

The vector-norm based truncation method is verified on a three-phase converter-based power system, whose dynamics can be modeled as an LTP system using HTFs. The diagram of the studied system is shown in Fig. 3, where two converters are considered. The verification is implemented in EMT simulations in MATLAB/Simulink. EMT simulation is sufficient for verification because it is a universal tool to conduct power system dynamic studies [25]. The control of the power converters and the harmonics of the grid voltage can lead to different strengths of frequency couplings in the linearized model, which can influence the truncation order and truncation errors.

In the studied system, the converter system seen at the point of connection (PoC) is assumed as a black-box system, as shown in the shaded area in Fig. 3. The detailed control schemes and system parameters for simulation implementations are provided in Appendix C. The frequency responses of the black-box system, i.e., the admittance HTF matrix, can be measured through the frequency scan at the PoC in EMT simulations. Since the converter ac side dynamics should be characterized by a two-port model, the ac admittance HTF model can be presented by a $2(2N+1)$-by-$2(2N+1)$ matrix with the square truncation, given the truncation order of N. The HTF model is assumed to be represented in the complex-valued $\alpha\beta$ frame in this work, where the two-port ac variables are defined as $\mathbf{v} := v_\alpha + jv_\beta$ and $e^{j2\theta_1}\mathbf{v}^* := e^{j2\theta_1}(v_\alpha - jv_\beta)$ [8]. With such complex-valued variable representations, the system fundamental frequency interval becomes $\Omega_0 = [0, 2\omega_1]$ where ω_1 is the line angular frequency of the three-phase power system. The ac admittance HTF can be represented by Fig. 4, which consists of four block HTF matrices, i.e., $\mathbf{y}_{11}$, $\mathbf{y}_{12}$, $\mathbf{y}_{21}$, and $\mathbf{y}_{22}$, as denoted by the four shaded areas. To realize the measurement, v_g is configured to represent the steady-state
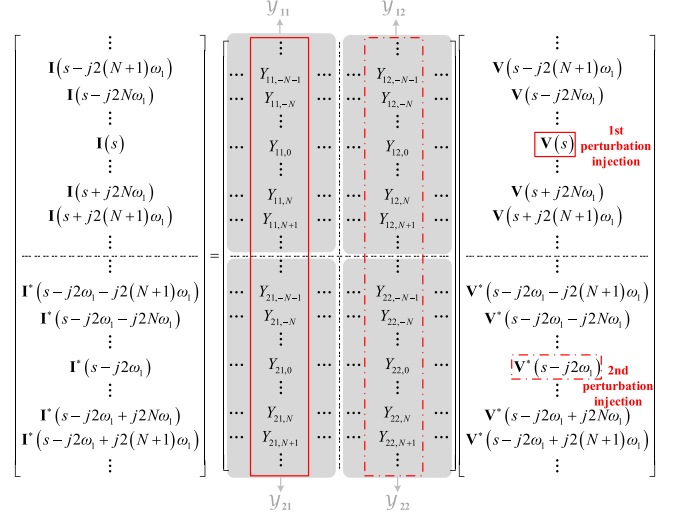
voltage at the PoC, and v_p is configured as the perturbation source. It can be seen from Fig. 4 that, in order to measure the central-column vectors of the four block HTF matrices, the single-frequency perturbation needs to be injected twice, for $\mathbf{v}$ and $e^{j2\theta_1}\mathbf{v}^*$, respectively. Then, the frequency responses of the corresponding column vectors can be calculated based on DFT analysis, whose elements are shown in the red solid and dash-dot boxes in Fig. 4. These elements will be further used for truncation analysis of the admittance HTF.

Since most truncation order selection approaches are not applicable without a state-space realization, and the H_∞-norm based approach requires more complicated frequency response measurement, which is less practical, the validation in case studies will not consider the comparisons with the existing approaches. Instead, the proposed truncation method is implemented by the two ways introduced in Section III-E for cross validations. The truncation will be analyzed for three cases:

- Case I: Converters are working in the balanced grid condition.
- Case II: Converters are working in the unbalanced grid condition (phase C short circuited at v_g), where the negative sequence voltage is introduced. The converters adopt conventional phase locked loops (PLLs) that cannot filter out the negative-sequence voltage component.
- Case III: Converters are working in the unbalanced grid condition (phase C short circuited at v_g), which is the same as Case II. Differently, the converters adopt advanced PLLs that can filter out the negative-sequence voltage component.

A. CASE I: BALANCED GRID CONDITION

The gain functions with different truncation orders under Case I are calculated based on the measured frequency responses, as shown in Fig. 5. It can be seen that the convergence of
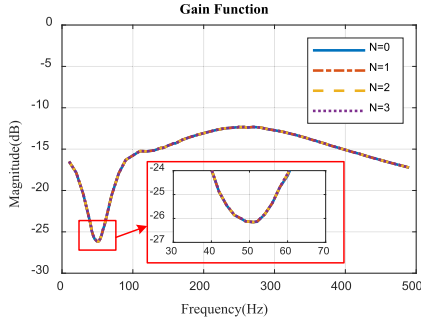
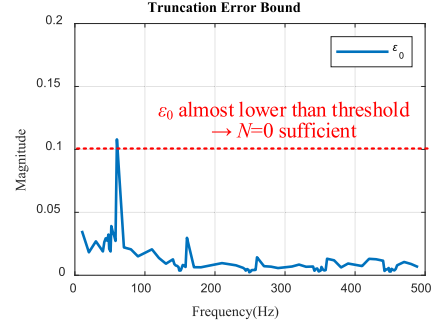**FIGURE 5.** Gain functions of the truncated admittance HTF model for Case I.

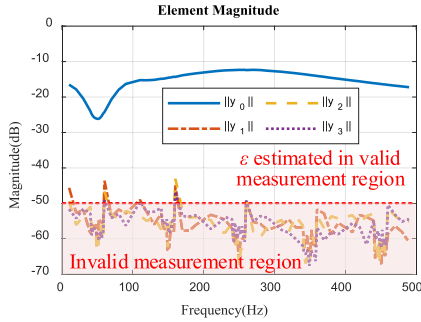**FIGURE 7.** Truncation error bound estimation of N = 0 for Case I.

FIGURE 6. Element magnitudes of different harmonic orders for Case I.
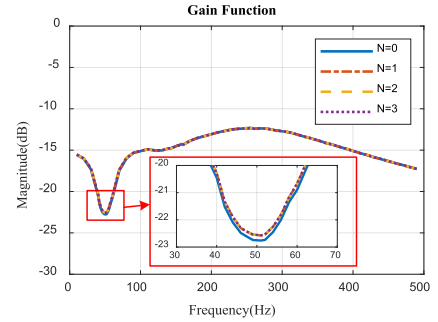

FIGURE 8. Gain functions of the truncated admittance HTF model for Case II.

the gain functions can be achieved with $N = 0$. Thus, the truncation order of zero is sufficient. It is indicated from this case that an LTI model is sufficient to characterize the two-port ac dynamics of the converter systems under balanced grid conditions.

The truncation error bound can be further estimated based on measured elements shown in Fig. 4. The element magnitudes of different harmonic orders (i.e., $\|y_k\|$) can be calculated based on the Frobenius norm given by

$$\|y_k\| := \sqrt{\sum_{i,j} \|y_{ij,k}\|^2} \tag{15}$$

where $\|y_{ij,k}\|$ is defined according to (13). The element magnitudes are plotted in Fig. 6. It can be seen that, for $k \geq 1$, $\|y_k\|$'s do not feature much difference around -50 dB and the curves are not smooth. It is implied that these measured responses are not accurate and reliable, because their values are too small. Therefore, the value of ε can only be estimated by $\|y_1\|/\|y_0\|$ in a valid measurement region, which is simply defined as the region whose magnitude is higher than -50 dB in this case. Although the obtained values of $\|y_1\|$ may not be precise around -50 dB, it can be judged from Fig. 6 that the decay rate of $\|y_1\|/\|y_0\|$ is much smaller than one, which ensures that the truncation error is sufficiently small according to (13). Taking $N = 0$ and assuming $\varepsilon = \max_{\omega \in \Omega_{\mathrm{VMR}}} \|y_1\|/\|y_0\|$ in the valid measurement region, where Ω_{VMR} is defined as the frequency range in which both $\|y_1\|$ and $\|y_0\|$ have

valid measurement values, the truncation error bound can be estimated as plotted in Fig. 7. If assuming a threshold of 0.1, it can be seen that the truncation error bound ε_0 is almost smaller than the threshold, thus $N = 0$ can be accepted for truncation. The truncation error bound analysis also verifies the truncation result obtained from Fig. 5.

B. CASE II: UNBALANCED GRID CONDITION WITH CONVENTIONAL PLL
Under Case II when the grid voltage is unbalanced, the truncation analysis of the admittance HTF model is conducted. The gain functions with different truncation orders are plotted in Fig. 8. From the zoomed in figure, the convergence of the gain function can be observed with $N = 1$.

The element magnitudes of different harmonic orders are calculated in Fig. 9. It can be seen that only the decay rates of $\|y_1\|/\|y_0\|$ and $\|y_2\|/\|y_1\|$ can be reliable, since their magnitudes have values in the valid measurement region, which can be well distinguished. The magnitudes of $\|y_2\|$ and $\|y_3\|$ are both too close to -50 dB, which cannot be well distinguished, indicating that the decay rate of $\|y_3\|/\|y_2\|$ is unreliable. Therefore, the decay rate upper bound is only estimated by $\varepsilon = \max_{\omega \in \Omega_{\mathrm{VMR}}} (\|y_1\|/\|y_0\|, \|y_2\|/\|y_1\|)$ for $N = 0$ or $\varepsilon = \max_{\omega \in \Omega_{\mathrm{VMR}}} \|y_2\|/\|y_1\|$ for $N = 1$ in the valid measurement region.

Consequently, the truncation error bounds ε_0 and ε_1 are estimated and plotted in Fig. 10. It can be seen that the
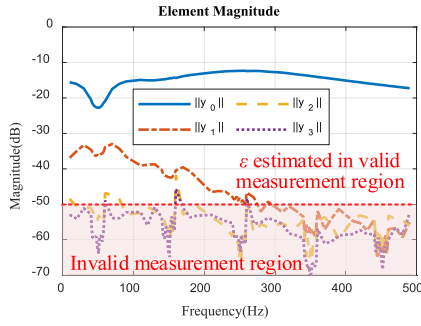
FIGURE 9. Element magnitudes of different harmonic orders for Case II.

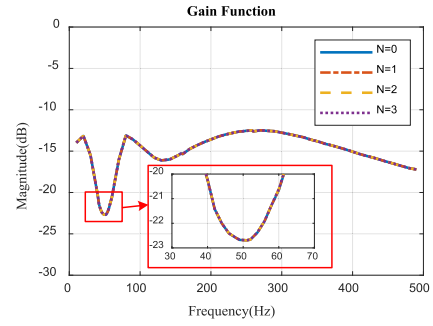**FIGURE 10.** Truncation error bound estimation of N = 0 and N = 1 for Case II.

truncation error bound ε_0 is much higher than the threshold around 50 Hz, thus $N = 0$ is insufficient for truncation. This explains why the gain functions of $N = 0$ and $N = 1$ have some difference at 50 Hz in Fig. 8. When the truncation order increases to $N = 1$, the truncation error bound ε_1 becomes smaller than the threshold, which is acceptable for truncation.

Compared with Case I, the truncation order is increased in this case due to the harmonic impact of the negative sequence voltage.

C. CASE III: UNBALANCED GRID CONDITION WITH ADVANCED PLL

The truncation analysis is conducted similarly under Case III. The gain functions, element magnitudes, and truncation error bounds are plotted in Figs. 11–13, respectively. It is found from Fig. 11 that when the advanced PLLs are adopted, the truncation order of $N = 0$ is already adequate. Comparing Figs. 9 and 12, it can be found that the magnitude of $\|y_1\|$ has been significantly reduced around 50 Hz and 150 Hz, which is resulted from the advanced PLL due to its mitigation of the negative-sequence voltage component. Consequently, the truncation error bound ε_0 is already almost smaller than the threshold, as shown in Fig. 13. Compared with ε_0, ε_1 does not decrease the error bound significantly. Thus, increasing the truncation order from $N = 0$ to $N = 1$ does not contribute to a more accurate HTF model, which agrees with the result in Fig. 11.
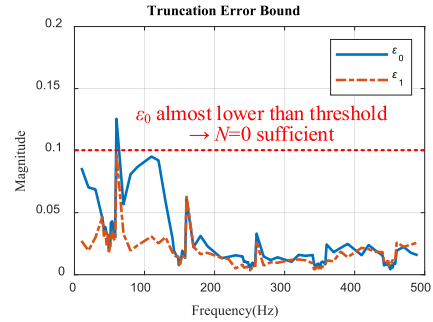

FIGURE 11. Gain functions of the truncated admittance HTF model for Case III.

FIGURE 12. Element magnitudes of different harmonic orders for Case III.

FIGURE 13. Truncation error bound estimation of N = 0 and N = 1 for Case III.

Comparing Case II and Case III, it is indicated that the converter control on the harmonic mitigation can result in a reduced-order modeling of the converter-based system. That is to say, truncation relying only on the system's steady-state harmonics like in [9]–[12] may result in a more conservative truncation order.

D. DISCUSSION

The above case studies show that the truncation result is influenced by not only the harmonic orders in the LTP system, e.g., how large the negative-sequence voltage component is, but also the harmonic mitigation control in converter systems. The resulted truncation order is around the same degree of

harmonic orders in the system, which is much less than the truncation order based on the HSS eigenvalue analysis (e.g., $N = 23$ given in [16]). This is because the HSS eigenvalue-based truncation requires to fold all the necessary poles into the fundamental frequency interval for dynamic analysis. The converter-based system may have some high-frequency poles/zeros, which cannot be folded into the fundamental frequency interval unless a very high truncation order is selected. However, these high-frequency poles/zeros are usually resulted from LTI parts of the system, which have already been characterized by the central diagonal of the HTF. Their dynamics can be easily analyzed by the LTI model (truncating the HTF with $N = 0$) defined in a wider frequency range. Therefore, the proposed method also results in much less truncation order compared with the HSS eigenvalue-based approach, which can simplify the HTF calculation.

IV. CONCLUSION

A vector-norm based truncation method has been proposed to select the truncation order of HTFs for "black-box" LTP systems. The method can be seen as a practical implementation of the skew truncation and can be easily implemented based on frequency-scan measurement. The truncation approach has been validated on a converter-based power system through the admittance measurement. It is found that the harmonic distortions in the three-phase system may increase the HTF truncation order, while the converter control has ability to decrease it thanks to the harmonic mitigation control. Thus, the truncation order of HTFs for LTP systems cannot be simply determined based on system steady-state harmonic orders.

APPENDICES
A. PROOF OF TRUNCATION ERROR BOUND BASED ON GAIN FUNCTION

$$\varepsilon_N(\omega) = \frac{\text{Gain}_\Delta(\omega)}{\text{Gain}_N(\omega)} = \frac{\sqrt{\|g_{N+1}(\omega)\|^2 + \|g_{N+2}(\omega)\|^2 + \cdots}}{\text{Gain}_N(\omega)}$$

$$= \frac{\|g_{N+1}(\omega)\|\sqrt{1 + \left(\frac{\|g_{N+2}(\omega)\|}{\|g_{N+1}(\omega)\|}\right)^2 + \left(\frac{\|g_{N+2}(\omega)\|}{\|g_{N+1}(\omega)\|} \cdot \frac{\|g_{N+3}(\omega)\|}{\|g_{N+2}(\omega)\|}\right)^2 + \cdots}}{\text{Gain}_N(\omega)}$$

$$\text{If } \frac{\|g_{k+1}(\omega)\|}{\|g_k(\omega)\|} = \sqrt{\frac{|G_{k+1}(j\omega)|^2 + |G_{-k-1}(j\omega)|^2}{|G_k(j\omega)|^2 + |G_{-k}(j\omega)|^2}}$$

$$\leq \varepsilon \text{ for } \forall k \geq N+1$$

$$\Rightarrow \quad \varepsilon_N(\omega) \leq \frac{\|g_{N+1}(\omega)\| \cdot \sqrt{1 + \varepsilon^2 + \varepsilon^4 + \cdots}}{\text{Gain}_N(\omega)}$$

$$= \frac{\|g_{N+1}(\omega)\|}{\text{Gain}_N(\omega)} \cdot \sqrt{\frac{1}{1-\varepsilon^2}}$$
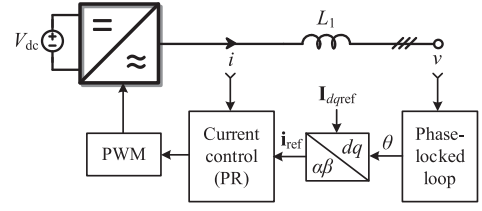

FIGURE 14. Control scheme of the converter.

B. PROOF OF SKEW TRUNCATION ERROR BOUND IN RELATION TO THE PROPOSED APPROACH

The H_2 norm for the skew truncation is defined by the following equation [22], which is bounded by the Frobenius norm of the HTF, i.e.,

$$\|G\|_{H_2}^2 = \frac{1}{2\pi} \int_{\Omega_0} \text{trace}[\boldsymbol{G}^*(j\omega')\boldsymbol{G}(j\omega')]d\omega'$$

$$\leq \frac{1}{T_p} \max_{\omega' \in \Omega_0} \sum_{k=-\infty}^{\infty} \|\text{Gain}^k(\omega')\|^2$$

where $T_p = 2\pi/\omega_p$.

Similarly, it holds that

$$\|G_N\|_{H_2}^2 \leq \frac{1}{T_p} \max_{\omega' \in \Omega_0} \sum_{k=-\infty}^{\infty} \left\|\text{Gain}_N^k(\omega')\right\|^2$$

$$\|G_\Delta\|_{H_2}^2 = \|G - G_N\|_{H_2}^2 \leq \frac{1}{T_p} \max_{\omega' \in \Omega_0} \sum_{k=-\infty}^{\infty} \left\|\text{Gain}_\Delta^k(\omega')\right\|^2$$

Based on (12) and (13), if $\varepsilon_N(\omega)$ is bounded by $\bar{\varepsilon}_N$, it holds that

$$\|\text{Gain}_\Delta(\omega)\|^2 \leq \bar{\varepsilon}_N^2 \|\text{Gain}_N(\omega)\|^2 \text{ where } \bar{\varepsilon}_N := \max_{\omega \in \mathbb{R}} \varepsilon_N(\omega)$$

Then, it can be derived that

$$\|G_\Delta\|_{H_2}^2 \leq \frac{1}{T_p} \max_{\omega' \in \Omega_0} \sum_{k=-\infty}^{\infty} \left\|\text{Gain}_\Delta^k(\omega')\right\|^2$$

$$\leq \frac{1}{T_p} \max_{\omega' \in \Omega_0} \sum_{k=-\infty}^{\infty} \bar{\varepsilon}_N^2 \left\|\text{Gain}_N^k(\omega')\right\|^2$$

$$= \bar{\varepsilon}_N^2 \frac{1}{T_p} \max_{\omega' \in \Omega_0} \sum_{k=-\infty}^{\infty} \left\|\text{Gain}_{N,k}(\omega')\right\|^2 = \bar{\varepsilon}_N^2 \|G_N\|_{H_2}^2$$

C. CONTROL SCHEMES AND SYSTEM PARAMETERS OF THE TESTED SYSTEM

The two converters adopt the typical grid-following control, whose control scheme is shown in Fig. 14, but the converter parameters are different. The two adopted PLLs are shown in Fig. 15. The circuit and control parameters are listed in Table 2.
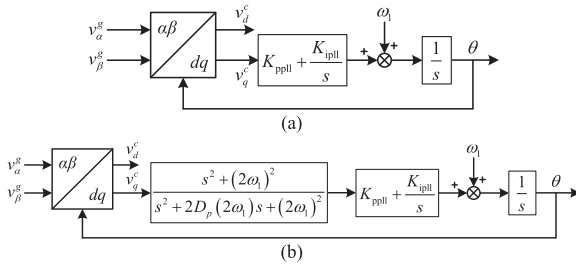
FIGURE 15. Control schemes of PLLs. (a) Conventional PLL; (b) Advanced PLL with a notch filter.

TABLE 2 Circuit and Control Parameters

Parameter	Value	Parameter	Value
V_g (line-line)	200 V_{RMS}	f_1	50 Hz
V_{dc}	700 V	V_p	10 V_{RMS}
L_{f1}	3 mH	C_{f1}	20 μF
L_{f2}	5 mH	C_{f2}	10 μF
L_{line1}	3 mH	L_{line2}	2 mH
L_{line}	3 mH	I_{qref1} / I_{qref2}	0 A
I_{dref1}	5 A	I_{dref2}	10 A
K_{pi1}	15	K_{ri1}	1516
K_{pi2}	25	K_{ri2}	2527
K_{ppll1} / K_{ppll2}	0.76	K_{ipll1} / K_{ipll2}	89.35
D_{p1} / D_{p2}	0.707	f_{s1} / f_{s2}	10 kHz

Note: Subscripts "1" and "2" denote the first and second converters, respectively. I_{dref} and I_{qref} are the current references in d and q axes. K_{pi} and K_{ri} are gains of the PR controller in current loop. K_{ppll} and K_{ipll} are gains of the PI controller in PLL. D_p is the damping ratio of the notch filter in the advanced PLL. f_1 is the line frequency and f_s is the switching and sampling frequency of converters.

REFERENCES

[1] A. I. Semlyen, "s-domain methodology for assessing the small signal stability of complex systems in nonsinusoidal steady state," *IEEE Trans. Power Syst.*, vol. 14, no. 1, pp. 132–137, Feb. 1999.

[2] E. Mollerstedt and B. Bernhardsson, "Out of control because of harmonics-an analysis of the harmonic response of an inverter locomotive," *IEEE Control Syst. Mag.*, vol. 20, no. 4, pp. 70–81, Aug. 2000.

[3] J. J. Rico, M. Madrigal, and E. Acha, "Dynamic harmonic evolution using the extended harmonic domain," *IEEE Trans. Power Del.*, vol. 18, no. 2, pp. 587–594, Apr. 2003.

[4] T. Noda, A. Semlyen, and R. Iravani, "Harmonic domain dynamic transfer function of a nonlinear time-periodic network," *IEEE Trans. Power Del.*, vol. 18, no. 4, pp. 1433–1441, Oct. 2003.

[5] J. Kwon, X. Wang, F. Blaabjerg, C. L. Bak, A. R. Wood, and N. R. Watson, "Linearized modeling methods of AC–DC converters for an accurate frequency response," *IEEE J. Emerg. Sel. Topics Power Electron.*, vol. 5, no. 4, pp. 1526–1541, Dec. 2017.

[6] A. Packard, K. Poolla, and R. Horowitz, "Dynamic systems and feedback class notes," Dept. Mech. Eng., Univ. California, Berkeley, CA, USA, 2005.

[7] N. M. Wereley, "Analysis and control of linear periodically time varying systems," Ph.D. dissertation, Dept. Aeronaut. Astronaut., MIT, 1991.

[8] Y. Liao and X. Wang, "Small-signal modeling of AC power electronic systems: Critical review and unified modeling," *IEEE Open J. Power Electron.*, vol. 2, pp. 424–439, 2021.

[9] V. Salis, A. Costabeber, S. M. Cox, F. Tardelli, and P. Zanchetta, "Experimental validation of harmonic impedance measurement and LTP nyquist criterion for stability analysis in power converter networks," *IEEE Trans. Power Electron.*, vol. 34, no. 8, pp. 7972–7982, Aug. 2019.

[10] S. R. Hall and N. M. Wereley, "Generalized nyquist stability criterion for linear time periodic systems," in *Proc. Amer. Control Conf.*, San Diego, CA, USA, 1990, pp. 1518–1525.

[11] Y. Liao, X. Wang, X. Yue, and L. Harnefors, "Complex-valued multifrequency admittance model of three-phase VSCs in unbalanced grids," *IEEE J. Emerg. Sel. Topics Power Electron.*, vol. 8, no. 2, pp. 1934–1946, Jun. 2020.

[12] H. Wu and X. Wang, "Dynamic impact of zero-sequence circulating current on modular multilevel converters: Complex-valued AC impedance modeling and analysis," *IEEE J. Emerg. Sel. Topics Power Electron.*, vol. 8, no. 2, pp. 1947–1963, Jun. 2020.

[13] P. C. Stefanov and A. M. Stankovic, "Modeling of UPFC operation under unbalanced conditions with dynamic phasors," *IEEE Trans. Power Syst.*, vol. 17, no. 2, pp. 395–403, May 2002.

[14] P. J. Hart, J. Goldman, R. H. Lasseter, and T. M. Jahns, "Impact of harmonics and unbalance on the dynamics of grid-forming, frequency-droop-controlled inverters," *IEEE J. Emerg. Sel. Topics Power Electron.*, vol. 8, no. 2, pp. 976–990, Jun. 2020.

[15] A. Jamshidifar and D. Jovcic, "Small-signal dynamic DQ model of modular multilevel converter for system studies," *IEEE Trans. Power Del.*, vol. 31, no. 1, pp. 191–199, Feb. 2016.

[16] V. Salis, A. Costabeber, S. M. Cox, and P. Zanchetta, "Stability assessment of power-converter-based AC systems by LTP theory: Eigenvalue analysis and harmonic impedance estimation," *IEEE J. Emerg. Sel. Topics Power Electron.*, vol. 5, no. 4, pp. 1513–1525, Dec. 2017.

[17] H. Yang, H. Just, M. Eggers, and S. Dieckerhoff, "Linear time-periodic theory based modeling and stability analysis of voltage source converters," *IEEE J. Emerg. Sel. Topics Power Electron.*, vol. 9, no. 3, pp. 3517–3529, Jun. 2021.

[18] P. D. Rua, O. C. Sakinci, and J. Beerten, "Comparative study of dynamic phasor and harmonic state-space modeling for small-signal stability analysis," *Elect. Power Syst. Res.*, vol. 189, no. 106626, pp. 1–8, Dec. 2020.

[19] H. Yang and S. Dieckerhoff, "Truncation order selection method for LTP-theory-based stability analysis of converter dominated power systems," *IEEE Trans. Power Electron.*, vol. 36, no. 11, pp. 12168–12172, Nov. 2021.

[20] J. Zhou and T. Hagiwara, "H2 and H∞ norm computations of linear continuous-time periodic systems via the skew analysis of frequency response operators," *Automatica*, vol. 38, pp. 1381–1387, Jan. 2002.

[21] N. M. Wereley and S. R. Hall, "Frequency response of linear time periodic systems," in *Proc. 29th IEEE Conf. Decis. Control*, Honolulu, HI, USA, 1990, vol. 6, pp. 3650–3655.

[22] H. Sandberg, E. Mollerstedt, and B. Bernhardsson, "Frequency-domain analysis of linear time-periodic systems," *IEEE Trans. Autom. Control*, vol. 50, no. 12, pp. 1971–1983, Dec. 2005.

[23] J. Zhou and T. Hagiwara, "Computing frequency response gains of linear continuous-time periodic systems," *IEE Proc. Control Theory Appl.*, vol. 148, no. 4, pp. 291–297, Jul. 2001.

[24] H. Sandberg, "On Floquet-Fourier realizations of linear time-periodic impulse responses," in *Proc. 45th IEEE Conf. Decis. Control*, 2006, pp. 1411–1416.

[25] N. R. Watson and J. Arrillaga, *Power Systems Electromagnetic Transients Simulation*, 2nd ed. IET Digital Library, 2018.

YICHENG LIAO (Member, IEEE) received the B.S. and M.S. degrees in electrical engineering from Southwest Jiaotong University, Chengdu, China, in 2015 and 2018, respectively, and the Ph.D. degree in energy technology from Aalborg University, Aalborg, Denmark, in 2021.

In July 2017, she was a Visiting Student with Ecole Polytechnique and French National Institute for Research in Digital Science and Technology, Paris, France. From September 2018 to July 2021, she was with the AAU Energy, Aalborg University, as a Research Assistant and later on as a Postdoc. From August 2021 to December 2021, she was a Postdoc with the School of Electrical Engineering and Computer Science, KTH Royal Institute of Technology, Stockholm, Sweden. Since January 2022, she has been a Power System Engineer with Elnetanalyse, Energinet, Denmark. Her research interests include the modeling, stability analysis, and control of power electronics-based power systems.

She was selected as the 2020 Outstanding Reviewer of the IEEE TRANSACTIONS ON POWER ELECTRONICS and the 2020 Star Reviewer of the IEEE JOURNAL OF EMERGING AND SELECTED TOPICS IN POWER ELECTRONICS. She was the recipient of the 2020 Top Download Paper Award in IEEE OPEN JOURNAL OF THE INDUSTRIAL ELECTRONICS SOCIETY and the 2021 Ph.D. Thesis Talk Award in IEEE Power Electronics Society.

HENRIK SANDBERG (Senior Member, IEEE) received the M.Sc. degree in engineering physics and the Ph.D. degree in automatic control from Lund University, Lund, Sweden, in 1999 and 2004, respectively.

He is currently a Professor with the Division of Decision and Control Systems, KTH Royal Institute of Technology, Stockholm, Sweden. From 2005 to 2007, he was a Postdoctoral Scholar with the California Institute of Technology, Pasadena, CA, USA. In 2013, he was a Visiting Scholar with the Laboratory for Information and Decision Systems, Massachusetts Institute of Technology, Cambridge, MA, USA. He has also held visiting appointments with Australian National University, Canberra, ACT, Australia, and the University of Melbourne, Melbourne, VIC, Australia. His current research interests include security of cyber-physical systems, power systems, model reduction, and fundamental limitations in control.

He was the recipient of the Best Student Paper Award from the IEEE Conference on Decision and Control in 2004, Ingvar Carlsson Award from the Swedish Foundation for Strategic Research in 2007, and a Consolidator Grant from the Swedish Research Council in 2016. He was on the editorial boards of the IEEE TRANSACTIONS ON AUTOMATIC CONTROL and *IFAC Journal Automatica*.

XIONGFEI WANG (Senior Member, IEEE) received the B.S. degree in electrical engineering from Yanshan University, Qinhuangdao, China, in 2006, the M.S. degree in electrical engineering from the Harbin Institute of Technology, Harbin, China, in 2008, and the Ph.D. degree in energy technology from Aalborg University, Aalborg, Denmark, in 2013.

Since 2009, he has been with the Department of Energy, Aalborg University, where he became an Assistant Professor in 2014, an Associate Professor in 2016, a Professor and the Leader of Electronic Power Grid Research Group in 2018. Since 2020, he has also been a Visiting Professor with the KTH Royal Institute of Technology, Stockholm, Sweden. His current research interests include modeling and control of power electronic converters and systems, stability and power quality of power-electronics-dominated power systems, and high-power converters.

He is the Co-Editor-in-Chief of the IEEE TRANSACTIONS ON POWER ELECTRONICS and as an Associate Editor for the IEEE JOURNAL OF EMERGING AND SELECTED TOPICS IN POWER ELECTRONICS (JESTPE). He was selected into Aalborg University Strategic Talent Management Program in 2016. He was the recipient of six prize paper awards in the IEEE Transactions and conferences, the 2018 Richard M. Bass Outstanding Young Power Electronics Engineer Award, 2019 IEEE PELS Sustainable Energy Systems Technical Achievement Award, 2020 IEEE Power & Energy Society Prize Paper Award, 2020 JESTPE Star Associate Editor Award, and Highly Cited Researcher in the Web of Science in 2019–2021.